Supporting Information

McCubbin et al. 10.1073/pnas.1006677107

SI Text

Characterization of SIMS Standards and 15404,51 Lithology. ***Electron probe microanalysis (EPMA).*** EPMA was employed for two different purposes in this study. The first was to analyze the three fluorapatite standards used for secondary ion mass spectrometry (SIMS) analysis to corroborate the SIMS calibration for fluorine and chlorine. The second purpose was to classify the lithologic clast in sample 15404,51. All the samples were analyzed with a JEOL JXA-8800L electron microprobe, housed at the Geophysical Laboratory in Washington, DC. An accelerating voltage of 15 kV and a nominal beam current of 15 nA were used for all analyses. The beam diameter for each analysis was 10 μm. The terrestrial apatite standards were analyzed for the elements Ca, P, F, Cl, Fe, Na, Mn, Mg, Si, Ce, and Y. Ca, P, and F were standardized using Durango apatite; Na and Cl were standardized using scapolite; Fe, Mn, Mg, and Si were standardized using a basaltic glass; and Ce and Y were standardized using the phosphates $CePO_4$ and YPO_4, respectively. The compositions of the terrestrial fluorapatite standards are presented in Table S1.

The fluorine analyses determined by electron probe microanalysis and reported in Table S1 may be higher than the actual amount of fluorine in the apatites because fluorine X-ray count rates can increase during electron beam exposure (i.e., refs. 1 and 2). The chlorine and fluorine concentrations determined by electron probe microanalysis for the apatite standards were used only as a comparison to the values obtained by SIMS (i.e., the electron microprobe values obtained for F and Cl were not used as the concentration of F and Cl in the SIMS standards).

For petrologic classification of the clast in 15404,51, the elements Si, Ti, Al, Cr, Fe, Mn, Mg, Ca, Na, and K were analyzed. Si and K were standardized using orthoclase, Ti and Fe were standardized using ilmenite, Al and Ca were standardized on anorthite, Cr and Mg were standardized on $MgCr_2O_4$, and Na was standardized using scapolite.

Hydrogen manometry. H_2 manometry was carried out at the Institute for Study of the Earth's Interior, Okayama University, on three natural terrestrial fluorapatites. The concentrations of OH in the fluorapatites were determined so that the apatites could be used for standardization of the ion microprobe. The three fluorapatites were from different localities, including Durango, Mexico, Eagle, Colorado, and Morocco. The OH concentrations (reported as the H_2O equivalent) determined by H manometry are presented in Table S1.

H_2 manometry was carried out using the following procedure. First, the fluorapatite samples were ground and sieved into a 0.038–0.075 mm size fraction for the analysis. Next, the ground sample powders (ranging in mass from 0.14985 to 0.20751 grams) were placed in an oven overnight at 110 °C and then stored in a P_2O_5 dry glove box (P_2O_5 was used as the desiccant). Before the analysis, empty Pt crucibles were placed in silica glass vessels and heated to 1,050 °C for 20 min under high vacuum to drive off surface-adsorbed contaminants. The Pt crucibles were then transferred to the dry glove box, and the sample powders were placed in the Pt crucibles and sealed in the silica glass vessels. The silica glass vessels were then connected to a high vacuum line and preheated at 200 °C under continuous evacuation for 2 hours with electrical resistance heaters to drive off any remaining adsorbed water. Subsequent to this step, each vessel was connected to the H-manometry line (one at a time), and the Pt crucible containing the sample was heated (~100 °C/min) from room temperature to 1,000 °C using an induction furnace. The sample was then held at 1,000 °C for 20 min. Degassing was monitored throughout the sample heating process with a Pirani gauge. Degassing typically started at around 300 °C and ended by approximately 900 °C. The released gas passed through a copper oxide furnace at 400 °C to oxidize any possible reduced species, and the gas was condensed using liquid nitrogen. The H_2O was then cryogenically purified within a mixture of acetone and $^{solid}CO_2$ (dry ice), and it was converted to H_2 in a uranium furnace at 700 °C. The H_2 gas was then transferred into two separate calibrated volumes by a Toepler pump, and the pressure of the H_2 gas was determined.

The two calibrated volumes resulted in two water concentrations for each analysis, which were averaged in order to determine the bulk water content. The two water concentrations for each measurement were within 54–60 ppm of each other for each analysis. The remaining analytical error of this technique lies within the uncertainty of the pressure measurement, which was typically between 100 and 260 ppm H_2O. The uncertainty of each analysis is reported in Table S1. Each of the analyses was corrected against a blank measurement, which typically resulted in corrections of 26–35 ppm H_2O.

Secondary processes that can perturb parental magmatic volatile signatures. Before the volatile abundance of the parental liquid (and hence the magmatic source region) can be determined from the analyzed apatite compositions, one must consider the affects of secondary processes that commonly perturb magmatic volatile abundances during crystallization. Secondary processes can include (but are not limited to) degassing, metasomatism, lithologic assimilation, and magma mixing.

Magmatic degassing is a secondary process that is likely experienced by all lunar magmas, as fluid saturation is eventually reached during crystallization of any volatile-bearing magma. Degassing of a magma will generally drive magmatic volatile contents towards fluorine-enriched (relative to water and chlorine) compositions because water and, to a lesser extent, chlorine would partition into the exsolved fluid/vapor phase, while fluorine is more compatible in the silicate liquid (as summarized by refs. 5–7). Consequently, apatites will yield compositions reflecting a drier and more chlorine-deficient parental magma if degassing has taken place. If metasomatism, lithologic assimilation, and/or magma mixing have occurred, magmatic volatile compositions can be driven in any direction depending on what is being mixed. Therefore, information about parental magmatic volatile contents cannot be extracted from apatite if this process has occurred.

Unfortunately, we cannot definitively determine whether any of these secondary processes have occurred for the samples studied here. For simplicity in modeling the parental magmatic water contents for comparison to the previous estimate of the bulk lunar water content (<1 ppb water; i.e., ref. 8), we assume here that secondary processes have not affected the magmas during crystallization of NWA 2977 or the lithic clast in 15404,51. However, because magmatic degassing likely occurred at some stage during the petrogenesis of our samples, the estimates of the parental magmatic water contents will represent lower limits.

1. McCubbin FM, et al. (2010) Detection of structurally bound hydroxyl in apatite from Apollo mare basalt 15058,128 using TOF-SIMS. *Am Mineral* 95, in press; doi: 10.2138/am.2010.3448).
2. Stormer JC, Pierson ML, Tacker RC (1993) Variation of F-X-ray and Cl-X-ray intensity due to anisotropic diffusion in apatite during electron-microprobe analysis. *Am Mineral* 78:641–648.
3. Jarosewich E, Nelen JA, Norberg JA (1980) Reference samples for electron microprobe analysis. *Geostandard Newslett* 4:43–47.
4. Shearer CK, Papike J (2005) Early crustal building processes on the Moon: Models for the petrogenesis of the magnesian suite. *Geochim Cosmochim Acta* 69:3445–3461.
5. Webster JD, Rebbert CR (1998) Experimental investigation of H_2O and Cl^- solubilities in F-enriched silicate liquids; implications for volatile saturation of topaz rhyolite magmas. *Contrib Mineral Petr* 132:198–207.
6. Piccoli PM, Candela PA (2002) in *Phosphates: Geochemical, Geobiological, and Materials Importance*, pp 255–292.
7. Aiuppa A, Baker DR, Webster JD (2009) Halogens in volcanic systems. *Chem Geol* 263:1–18.
8. Taylor SR, Pieters CM, MacPherson GJ (2006) in *New Views of the Moon*, Mineralogical Society of America, Chantilly, VA, pp 657–704.

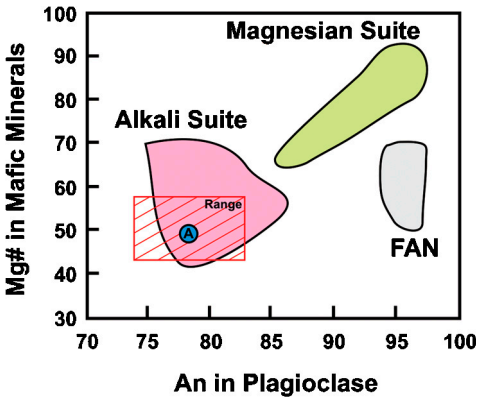

Fig. S1. Plot of anorthite content in plagioclase vs. Mg number of coexisting ferromagnesian silicates for ferroan anorthosites (FAN), the magnesian suite, and the alkali suite adapted from ref. 4. The average composition of pyroxene and plagioclase grains from the lithic clast 15404,51 (determined by EPMA) is plotted as a blue circle with the black letter A. The range in pyroxene and plagioclase values is indicated by the red box. This plot supports assigning the lithic clast in 15404,51 to the alkali suite.

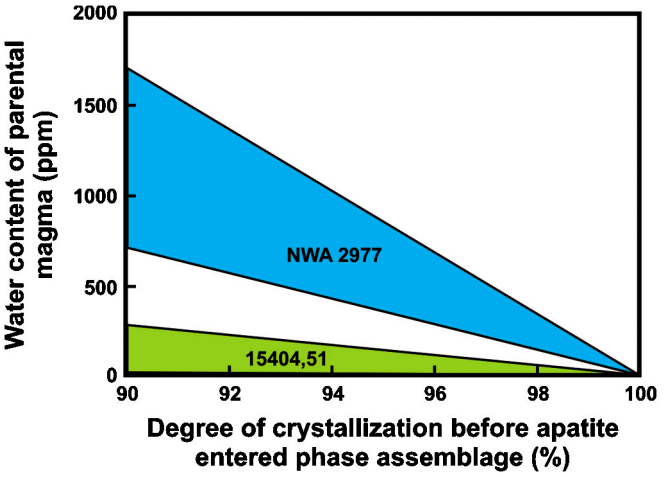

Fig. S2. Computed range of parental magmatic water contents for NWA 2977 and the alkali-suite clast in 15404,51. The water contents were calculated as a function of the percentage of crystallization before apatite entered the phase assemblage. The upper and lower lines for each range represent the calculated range in magmatic water contents at the time of apatite crystallization for each of the samples.

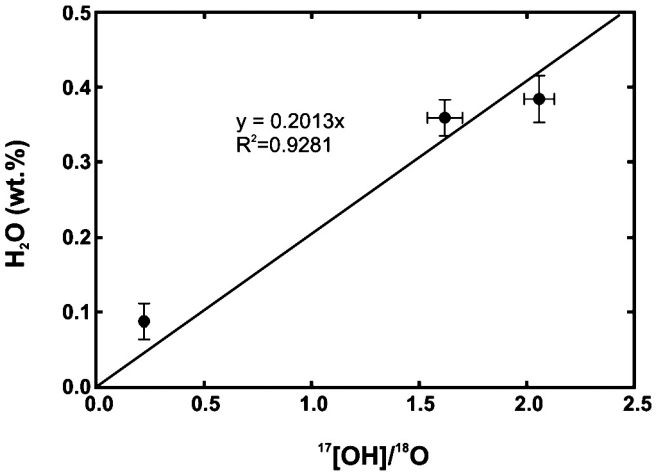

Fig. S3. Calibration curve determined for quantifying water contents of apatite by SIMS. The data points used to construct the curve were from our three terrestrial apatite standards (Table S1). The water contents for these apatite grains were determined by H manometry. The regression line is forced to the origin because the detection limit of our analysis routine is approximately 3 ppm H_2O. The discrepancy between the data point with the lowest water content (Durango apatite) and our regression line could be explained by the presence of minor fluid inclusions in the apatite that were not driven off during the initial drying steps before analysis by H manometry. The 2σ error for the slope of the calibration curve is about 17% (i.e., $m = 0.20 \pm 0.03$).

Table S1. Chemical analyses of terrestrial apatite standards

Oxide (wt%)	Durango	Colorado	Morocco
P_2O_5	40.1 (4)	40.8 (4)	40.5 (2)
SiO_2	0.35 (2)	0.26 (2)	0.44 (2)
Ce_2O_3	0.64 (4)	0.58 (6)	0.29 (4)
Y_2O_3	0.08 (3)	0.05 (3)	0.06 (2)
FeO	0.03 (2)	0.07 (2)	0.03 (2)
MnO	0.01 (1)	0.08 (2)	0.02 (1)
MgO	0.01 (1)	0.01 (1)	0.00 (0)
CaO	54.4 (2)	54.6 (2)	55.2 (2)
Na_2O	0.26 (5)	0.09 (1)	0.06 (1)
H_2O*	0.09 (2)	0.36 (2)	0.38 (3)
F	4.03†	2.6 (1)	2.5 (1)
Cl	0.45 (6)	0.95 (3)	0.41 (2)
$-O = F + Cl$	1.80	1.32	1.15
Total	98.65	99.13	98.74
Structural formulas based on 13 anions			
P	2.94	2.96	2.93
Si	0.03	0.02	0.04
Ce	0.02	0.02	0.01
Y	0.00	0.00	0.00
Fe	0.00	0.01	0.00
Mn	0.00	0.01	0.00
Mg	0.00	0.00	0.00
Ca	5.04	5.01	5.07
Na	0.04	0.01	0.01
F	1.10†	0.71	0.68
Cl	0.07	0.14	0.06
OH	0.05	0.21	0.22
Cation sum	8.07	8.04	8.06
X-site sum	1.22	1.06	0.96

Data collected by EPMA unless otherwise noted.

*Reported H_2O value determined by H manometry.

†Analysis experienced fluorine count rate increase during the analysis (i.e., refs. 1 and 2); therefore, the reported value is too high. Published Durango apatite has 3.53 wt% fluorine (3). The parenthetical numbers represent the uncertainty in the last digit of each reported value.